NUCLEAR THEORY, Vol. 42 (2025)
eds. M. Gaidarov, N. Minkov, Heron Press, Sofia

The Significance of the Quasiparticle-Phonon Model for the Study of Nuclear Structure and Nuclear Reactions

N. Tsoneva[1]

[1]Extreme Light Infrastructure-Nuclear Physics (ELI-NP)/Horia Hulubei National Institute for Physics and Nuclear Engineering (IFIN-HH), No. 30, Reactorului Street, Bucharest-Magurele, 077125, Romania

Abstract. A theoretical method based on energy-density functional (EDF) theory and the quasiparticle-phonon model (QPM) was developed, which includes a self-consistent mean field and multi-configuration mixing for the nuclear excited states consisting of up to three-phonon configurations. The method is applied to investigate nuclear two-phonon states, pygmy and giant resonances in a unified manner and to predict new excitation modes. A systematic comparison between quasiparticle-random-phase approximation (QRPA) and three-phonon QPM calculations in different nuclei shows that the behavior of the γ-strength function at low energies is influenced by the competition between static and dynamic effects. In the case of dipole excitations, these effects lead to a redistribution and fragmentation of the electric dipole strength at low energies, with particular emphasis on 1^- states with neutron one-particle-one-hole components identified with the pygmy dipole resonance (PDR). The latter serve as doorway states common to the neutron and γ channels in (n, γ) reactions and are expected to strongly influence isotope production in explosive stellar environments. Recently, the EDF+QPM approach has been successfully used to calculate branching ratios in the double γ-decay of nuclear isomer states and to interpret new experiments.

1 Introduction

This manuscript is dedicated to the 100th anniversary of the birth of Prof. V. Soloviev, the founder of QPM [1, 2], and highlights our long-term research experience with his theory for studying the nuclear structure of atomic nuclei. Over the years, QPM has become one of the most powerful theoretical models for comprehensive studies of nuclear excitations and has been used intensively in recent decades for a precise description of experimental data [3, 4] which is possible thanks to the development of modern computational resources.

The development of experimental facilities for radioactive nuclear beams opens the possibility of investigating unknown regions of exotic nuclei far from the valley of β-stability providing new insights into the isospin dynamics of nuclear matter. One of the most interesting discoveries related to skin oscillations

in stable and unstable neutron-excess nuclei is the "pygmy" dipole resonance (PDR) [4–11].

As a further extension of QPM theory, we have developed a theoretical approach based on EDF and QPM, which includes up to three-phonon configurations [4, 6, 7]. The main advantages of the method lie in its self-consistent mean-field (MF) and multi-configuration mixing, which are crucial for the systematic, unified study of nuclear low-energy excitations, as well as pygmy and giant resonances. In particular, the theoretical approach has proven to be very successful in predicting new excitation modes, especially the pygmy dipole [4,6] and quadrupole resonances [12, 13], which have also been observed experimentally [14, 15].

The origin of the PDR is still not fully understood. However, the currently available experimental and theoretical evidences from studies of (d,p), (d,pγ) and (p,d) reaction cross sections support the idea that the mode is generated by a vibration of the neutron skin against the isospin-symmetric nucleus [16, 17]. Furthermore, systematic studies of nuclear isotonic and isotopic chains of nuclei have established a correlation between the overall strength of the PDR and the thickness of the nuclear skin [6, 7, 9]. In general, the PDR appears as an additional component of the dipole strength in the neutron threshold region and is located above the low-energy tail of the giant dipole resonance (GDR), classically represented by a Lorentzian form [9]. However, it should be noted that not all of the observed strength in the PDR region is related to neutron skin oscillations. EDF+QPM calculations show that the PDR strength associated with neutron oscillations is very weak, about 1% of the energy-weighted-sum rule (EWSR), compared to the GDR, which dominates the electric dipole (E1) strength in atomic nuclei [18, 19].

Recent studies of nuclear reactions of astrophysical interest show that the reaction cross-sections strongly depend on the low-energy part of the electromagnetic strength function and the PDR which is connected to the dipole photoabsorption cross section [11, 20, 21]. The PDR can dramatically increase the capture reaction rates of neutrons and other particles important for the nucleosynthesis of heavier elements in stellar environments [11, 20].

Over the years, QPM theory has also been widely used in studies of two-phonon states of quadrupole-quadrupole, quadrupole-octopole multiplets of nuclear low-energy excited states. Of particular interest is the quadrupole-octupole 1^- state, associated with the coupling of collective 2^+_1 and 3^-_1 phonons ([3, 6, 22–25]). Typically, these 1^- states have only a very small strength, on the order of 10^{-3} W.u., but can serve as a very sensitive tool for demonstrating the reliability of nuclear structure models.

Recently, the EDF+QPM approach was used to describe the double-gamma decay of ^{137m}Ba [26]. Theoretically, we confirm the experimental observation of the double-photon-to-single-photon branching ratio of 2.62 10^{-6} (30)(exp.) and 3.73 10^{-6} (EDF+QPM). This remarkable agreement provides strong evidence for the reliability of our theoretical approach.

2 The Theoretical EDF+QPM Approach

Our theoretical approach is based on self-consistent energy-density functional theory (EDF) and the quasiparticle-phonon model (QPM) (EDF+QPM). Some of the main advantages of the EDF+QPM approach compared to other theoretical models are, first, the self-consistent determination of the nuclear ground state and, second, the description of the excited nuclear states in a large model configuration space, including up to three-phonon configurations.

The model Hamiltonian [1, 6] is given by:

$$H = H_{MF} + H_{res}\,, \tag{1}$$

where H_{MF} is a mean-field part and H_{res} stands for the residual interaction.

The mean-field (MF) part H_{MF} is treated by self-consistent Skyrme Hartree-Fock-Bogoliubov (HFB) theory described in [4, 27]. The pure HFB picture is in fact extended beyond MF by dynamical self-energies, hence incorporating a more detailed spectral description of nuclear spectra. The procedure allows us to account in a self-consistent manner for nuclear binding energies and other ground-state properties of nuclei like the charge radii and the neutron skin thickness [4, 7, 27].

The nuclear excited states are calculated with a residual interaction which is based on the QPM formalism [1, 2]:

$$H_{res} = H_M^{ph} + H_{SM}^{ph} + H_M^{pp}\,, \tag{2}$$

where effective interactions are implemented to account for the interaction between the quasiparticles. The terms H_M^{ph}, H_{SM}^{ph} and H_M^{pp} are taken as a sum of isoscalar and isovector separable multipole and spin-multipole interactions in the particle-hole ($p-h$) and multipole pairing interaction in the particle-particle ($p-p$) channels, respectively [1]. The model parameters are fixed empirically in such a way that the properties of the lowest-lying collective states and giant resonances are described accurately [28].

The nuclear excitations are expressed in terms of quasiparticle-random-phase-approximation (QRPA) phonons,

$$Q^+_{\lambda\mu i} = \frac{1}{2}\sum_{jj'}\Big(\psi^{\lambda i}_{jj'}A^+_{\lambda\mu}(jj') - \varphi^{\lambda i}_{jj'}\widetilde{A}_{\lambda\mu}(jj')\Big), \tag{3}$$

where the set of quantum numbers $j \equiv (nljm\tau)$ label single-nucleon states, and $A^+_{\lambda\mu}$ and $\widetilde{A}_{\lambda\mu}$ are the time-forward and time-backward two-quasiparticle (2QP) operators, creating or annihilating two quasiparticles coupled to a total angular momentum λ with projection μ. The excitation energies of the phonons and the time-forward and time-backward amplitudes $\psi^{\lambda i}_{j_1j_2}$ and $\varphi^{\lambda i}_{j_1j_2}$ in Eq. (3) are determined by solving QRPA equations [1, 2].

Thus, for spherical even-even nuclei the model Hamiltonian is diagonalized on an orthonormal set of wave functions constructed from one-, two- and three-phonon configurations [3, 22, 29]:

$$\Psi_\nu(JM) = \Bigg\{ \sum_i R_i(J\nu) Q^+_{JMi} + \sum_{\substack{\lambda_1 i_1 \\ \lambda_2 i_2}} P^{\lambda_1 i_1}_{\lambda_2 i_2}(J\nu) \left[Q^+_{\lambda_1 \mu_1 i_1} \times Q^+_{\lambda_2 \mu_2 i_2} \right]_{JM}$$

$$+ \sum_{\substack{\lambda_1 i_1 \lambda_2 i_2 \\ \lambda_3 i_3 I}} T^{\lambda_1 i_1 \lambda_2 i_2 I}_{\lambda_3 i_3}(J\nu) \left[[Q^+_{\lambda_1 \mu_1 i_1} \otimes Q^+_{\lambda_2 \mu_2 i_2}]_{IK} \otimes Q^+_{\lambda_3 \mu_3 i_3} \right]_{JM} \Bigg\} \Psi_0 \,, \quad (4)$$

where R, P and T are unknown amplitudes, ν labels the number of the excited states, and Ψ_0 is the ground state wave function of the even-even nucleus (phonon vacuum).

The electromagnetic transition matrix elements are calculated for transition operators including the interaction of quasiparticles and phonons [3, 22] where exact commutation relations are implemented which is a necessary condition in order to satisfy the Pauli principle.

Recently, a theoretical approach combining EDF + QPM theory with the nuclear reaction model (EDF + QPM + reaction) was developed to consistently derive (d,p) cross sections, γ decay branchings, (d,pγ) yields, and energy-integrated (γ,γ') cross sections [16, 17]. The theory was first applied in the calculation of spectroscopic factors of nuclear 1^- excited states of ^{120}Sn and ^{208}Pb populated by the ^{119}Sn(d,pγ)^{120}Sn and ^{207}Pb(d,p)^{208}Pb reactions [16, 17].

3 Discussion and Results

3.1 EDF+QPM studies of two-phonon 1^- states

Detailed theoretical descriptions of two-phonon 1^- states related to members of quadrupole-octupole $(2^+_1 \otimes 3^-_1)_{1^-_1}$ multiplet are obtained in the frame of the QPM which has been intensively applied in studies of multi-phonon states ([6, 22–24]).

The structure of the lowest-lying 1^- state (candidate for the two-phonon $(2^+_1 \otimes 3^-_1)_{1^-_1}$ 1^- state) of ^{88}Sr has been studied in the frame of EDF+QPM ([25]). According to the signatures of two-phonon states, an excitation energy of the two-phonon (2ph) 1^- state of ^{88}Sr is E(1^-_{2ph})$\approx$ E(2^+_1)+ E(3^-_1) = 1836 keV + 2734 keV = 4570 keV. However, for unambiguous identification, the reduced decay strengths of a harmonically coupled 1^- two-phonon state must satisfy the following relations: $B(E3, 1^-_{2ph} \longrightarrow 2^+_1) = B(E3, 3^-_1 \longrightarrow g.s.)$ and $B(E2, 1^-_{2ph} \longrightarrow 3^-_1) = B(E2, 2^+_1 \longrightarrow g.s.)$. A comparison of the EDF+QPM theory and the available experimental data is shown in Table 1. The QPM calculations are performed in a three-phonon model space ([25]). In the QPM calculations, the wave function of the calculated 1^-_1 state contains about 90%$(2^+_1 \otimes 3^-_1)$

Table 1. Comparison of experimental results to theoretical calculations within the EDF+QPM for ^{88}Sr. The experimental data are taken from ^{a} [25] and ^{b} [30]

	Experiment	QPM
$E_x(1_1^-)$ [MeV]	4.742^{a,b}	4.603
$E_x(2_1^+)$ [MeV]	1.836^{a,b}	1.830
$E_x(3_1^-)$ [MeV]	2.734^{a,b}	2.760
$B(E1, 1^- \rightarrow 0_1^+)$ [mW.u.]	0.93(12)^{a}	0.96
$B(E1, 3_1^- \rightarrow 2_1^+)$ [mW.u.]	0.66(5)^{b}	1.1
$B(E2, 2_1^+ \rightarrow 0_1^+)$ [W.u.]	7.6(4)^{b}	8.0
$B(E2, 1^- \rightarrow 3_1^-)$ [W.u.]	8.0(12)^{a}	8.1
$B(E3, 3_1^- \rightarrow 0_1^+)$ [W.u.]	22.6(21)^{b}	19.5
$B(E3, 1^- \rightarrow 2_1^+)$ [W.u.]	—	18.7
$B(E2, 1_1^- \rightarrow 3_1^-)/B(E2, 2_1^+ \rightarrow g.s.)$	1.06(17)^{a}	1.01
$B(E3, 1_1^- \rightarrow 2_1^+)/B(E3, 3_1^- \rightarrow g.s.)$	—	0.96

component and $7\%(1_3^-)$ QRPA state, which is an almost pure neutron QRPA state associated with the excitation of the PDR mode in this nucleus. Due to the one-phonon and two-phonon components in the structure of the 1_1^- state, anharmonicity effects shift the excitation energy of the state to lower excitation energies with respect to the pure harmonic expectation energy resulting from the sum of the energies of the QRPA 2_1^+ and 3_1^- states ([25]). The computed transition strengths for the 1_1^- and 2_1^+ states and their ratios are in remarkable agreement to the experimental values and are summarized in Table 1. The decay strengths for both the $1_1^- \rightarrow 0_1^+$ and the $1_1^- \rightarrow 3_1^-$ transitions and B(E2) ratios are in excellent agreement with the experimental data, which confirm the interpretation of the 1_{2ph}^- state as a two-phonon $(2_1^+ \otimes 3_1^-)_{1_1^-}$ state in ^{88}Sr [25]. Due to the dominant competition from the E1 transition, it is experimentally difficult to determine the contribution of E3 transition to the $1_{2ph}^- \longrightarrow 2_1^+$ decay ([25]). However, EDF+QPM calculations of B(E3, $1_{2ph}^- \longrightarrow 2_1^+$), B(E3, $3_1^- \longrightarrow$ g.s.) and their ratio are made. The obtained theoretical results are presented in the Table 1, where they play the role of predicting the value of B(E3, $1_{2ph}^- \longrightarrow 2_1^+$). The resulting ratio for the E3 transitions is 0.96. This theoretical result is a strong argument to confirm the two-phonon $(2_1^+ \otimes 3_1^-)$ nature of 1_1^- in ^{88}Sr.

3.2 EDF+QPM systematic study of the PDR in different isotopic and isotonic chains

Our first theoretical studies on spectral distributions of low-energy dipole states with respect to the PDR were performed on tin isotopes, $^{100\div132}$Sn, which represent an interesting probe for the systematic investigation of the evolution of nuclear dipole strength as a function of neutron excess [6, 7]. Our EDF+QRPA calculations clearly show that the PDR strength increases with increasing neu-

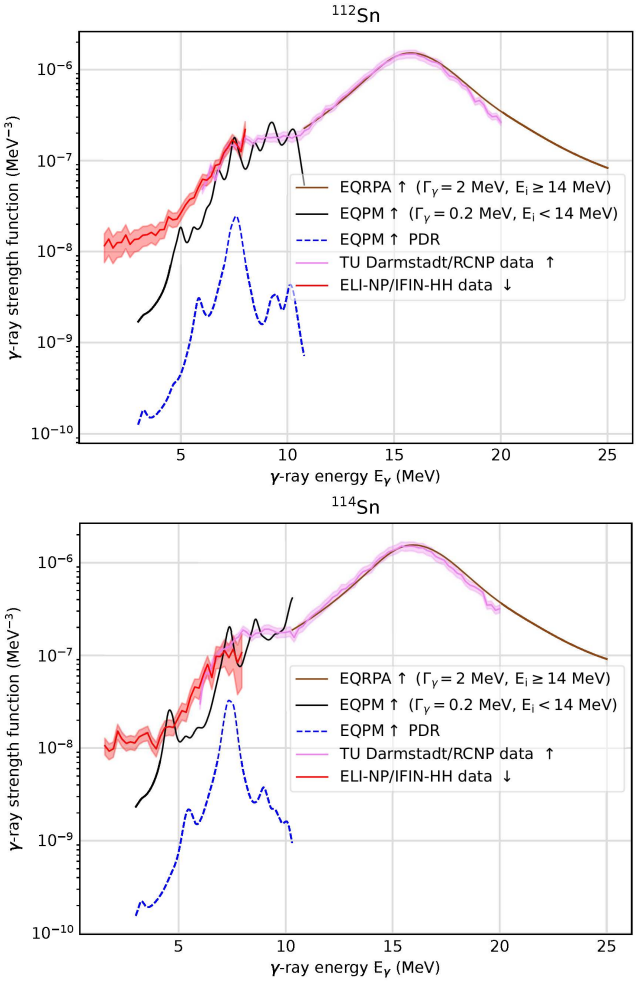

Figure 1. Qualitative comparison of the experimental γ-ray strength functions of ^{112}Sn (top) and ^{114}Sn (bottom), including also the ELI-NP/IFIN-HH data reported in [19] (red) as well as the data collected at RCNP by TU Darmstadt ([19]) (green) together with the calculated strengths from the QRPA (brown) and QPM (black, blue). The QRPA calculations have been smeared with a width of Γ_γ = 2 MeV and the EDF+QPM calculations have been smeared with a width of Γ_γ = 0.2 MeV. For the QRPA results, only states, i, with en energy larger than E_i = 14 MeV are included and for the EDF+QPM results only states with an energy less than E_i = 14 MeV are included. Note that the theoretical results have been renormalized for comparison to account for the long tails introduced during the Lorentzian smearing. Also note that the theoretical results and the TU Darmstadt data are for excitation strength (↑) while our data is for the decay strength (↓) ([18, 19]).

tron number and the corresponding neutron skin thickness, which is expressed as the difference between the root-mean-square radii of neutrons and protons. Similar relationships are found for Pb isotopes, N=50, 82 isotopes, and other neutron-excess nuclei. Experimentally, the E1 strength below the neutron separation energy in ^{116,124}Sn isotopes was investigated using a partially linearly polarized bremsstrahlung beam [31]. This experiment showed that the E1 strength in ^{124}Sn was significantly larger than that observed for ^{116}Sn.

For measuring γ-strength functions (gSF) and nuclear level densities (NLD) below the neutron separation threshold in ^{112,114}Sn, the Oslo method has been used [19] . We pointed out in the previous sections that the observed E1 strength at low energy does not correspond unambiguously to the neutron PDR mode, but contains an admixture of the low-energy tail of the GDR as well as contributions related to the coupling between multipoles with higher angular momentum. In this context, the EDF+QPM approach is able to consistently account for these features of the E1 spectra. The theoretical results for the dipole response below the neutron threshold in ^{112,114}Sn are shown in Figure 1. From the analysis of our QRPA calculations, it is found that the 1^- states at E$^*\approx$7-8 MeV in ^{112,114}Sn have a nearly pure neutron structure associated with the PDR in tin isotopes ([4, 7]). However, EDF+QPM calculations show that the total PDR strength increases with increasing neutron number, from 4.38 mb MeV (^{112}Sn) (0.26% of TRK EWSR) to 4.70 mb MeV (^{114}Sn) (0.28% of TRK EWSR), as expected, while the total low-energy dipole strength in ^{114}Sn decreases relative to ^{112}Sn due to the mixing of more complex configurations and GDR [18, 19]. The good overall agreement between the predicted total subthreshold E1 strengths of EDF+QPM and the experiment in ^{112,114}Sn suggests that in these nuclei the properties of the low-energy E1 spectra and the PDR are well defined.

3.2.1 Single-particle structure of PDR in double-magic ^{208}Pb

Our recent studies of low-energy excitations in lead isotopes: ^{204,206,208}Pb (N/Z>1) show the formation of a neutron skin [11, 16, 32]. It is observed that nuclear dipole excitations, especially at low energies in these nuclei, react sensitively to the presence of a neutron skin and can be related to the vibrations of extra neutrons with respect to an isospin symmetric nuclear core and the PDR.

The first comprehensive investigation of the single-particle character of the PDR in ^{208}Pb on the basis of new experimental data and their theoretical explanation is discussed in Ref. [16]. Theoretical predictions from EDF+QPM and the large-scale shell model (LSSM) are compared with new data from (d,p) and resonant proton scattering experiments. The latter allow the distinction of the two different transfer configurations by which 1^- states of ^{208}Pb can be populated from the J$^\pi$=1/2$^-$ ground state of ^{207}Pb; namely $(3p_{1/2})^{-1}(4s_{1/2})^{+1}$ (l=0), and $(3p_{1/2})^{-1}(3d_{3/2})^{+1}$ (l=2). The (d,p) strength pattern is dominated by the two strongly populated 1^- states at 5292 and 5947 keV, corresponding to the major fragments of the $(3p_{1/2})^{-1}(4s_{1/2})^{+1}$ [S=0.77(4)] and $(3p_{1/2})^{-1}(3d_{3/2})^{+1}$

[S=0.66(4)] neutron $1p-1h$ strength, respectively [16]. The differential cross sections $d\sigma/d\Omega$, predicted theoretical spectroscopic factors, i.e., the overlap of the ^{207}Pb ground state with excited 1^- states in ^{208}Pb when adding a neutron, were combined with the DWBA calculations. Unprecedented access to the theoretical wave functions demonstrating the $1p-1h$ neutron origin of the PDR in ^{208}Pb has been achieved. The comparison of EDF + QPM calculations shows that the model was able to account the main features of the (d,p) data. In particular, EDF+QPM predicts two dominant $(3p_{1/2})^{-1}(4s_{1/2})^{+1}$ [$S_{5.32MeV}$=0.92] and $(3p_{1/2})^{-1}(3d_{3/2})^{+1}$ [$S_{6.12MeV}$=0.68] fragments in excellent agreement with experiment [16]. For the total (d,p) cross section, the obtained EDF+QPM value is $\Sigma\sigma_{(d,p)(QPM)}$= 1676 μb which is also in very good agreement with experimental data of total $\Sigma\sigma_{(d,p)(exp.)}$ which can be taken as a sum of $\sum_{\leq S_n}\sigma_{(d,p)(exp.)}$= 1524(17) μb below and $\sum_{\geq S_n}\sigma_{(d,p)(exp.)}$= 254(9) μb above the neutron threshold S_n, respectively [17].However, EDF+QPM underestimates the observed strength above S_n. Due to the doubly magic nature of ^{208}Pb, the $1p-1h$ structure of the QRPA phonons dominates the configuration mixing and polarization contributions (cf. [11]).

3.2.2 Single-particle structure of PDR in semi-magic ^{120}Sn

In this section, we report on EDF+QPM calculations of single-particle structure of the PDR in semi-magic nucleus ^{120}Sn. In contrast to the case of the double-magic ^{208}Pb nucleus, the PDR in an open-shell nucleus ^{120}Sn is characterized by a much higher level density. In comparison, the ^{119}Sn(d,pγ)^{120}Sn reaction is studied in a novel experiment performed at the University of Cologne with the combined SONIC@HORUS setup for coincident particle-spectroscopy [17]. In order to describe the observed fragmentation pattern of the PDR mode in semi-magic nucleus ^{120}Sn, one must go beyond QRPA and to take into account the interaction between quasiparticles and phonons. That is achieved by the three-phonon QPM approach, introduced in Section 2. The ^{119}Sn target is assumed to be a pure $3s_{1/2}$ hole relative to the ^{120}Sn "core" [17]. Within this approximation, the ^{119}Sn$(d,p)^{120}$Sn reaction populates QPM 1^- states that contain $3p_{1/2}$ and $3p_{3/2}$ one-quasiparticle states, i.e., states with neutron $(3s_{1/2})^{-1}(3p_{1/2})^{+1}$ and $(3s_{1/2})^{-1}(3p_{3/2})^{+1}$ 1p-1h components. The corresponding angular differential cross section populating a QPM 1^- state ν in a one-step process results from the coherent contribution of these two components Since ^{120}Sn, in contrast to ^{208}Pb, is an open-neutron-shell nucleus (N = 70), two- and three-phonon confgurations already contribute at lower energies (compare Figure 1 and Figure 2). Below 7 MeV, one-phonon confgurations dominate the picture though. Above 7 MeV, two-phonon and three-phonon contributions begin to contribute signifcantly to the spectral distribution. The theoretical results of (d,pγ) yields, and energy-integrated (γ, γ') cross-sections in ^{120}Sn are shown in Figure 2 and they are found in very good agreement with the novel (d,pγ) experiment from Ref. [17]. The theoretical (d,pγ) strength is fragmented at lower energies and it reproduces

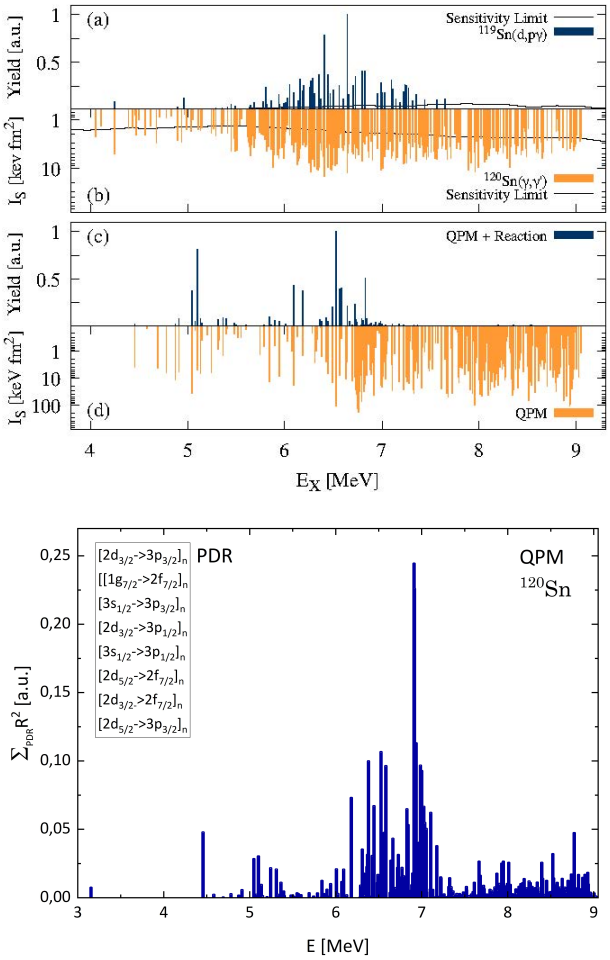

Figure 2. Top:(a) relative γ-ray yields from $^{119}Sn(d,p\gamma)$ and (b) energy integrated cross sections I_S for $^{120}Sn(\gamma,\gamma')$. All transitions shown in panel (a) were also observed in the NRF experiment. Sensitivity limits are based on a maximum error on the peak area of 30%. (c) relative $^{119}Sn(d,p\gamma)$ yields from the EQPM+Reaction formalism and (d) predicted energy integrated cross sections, both taking into account γ-decay branching predicted by the EDF+QPM. Theoretical (d,p) cross sections were calculated at scattering angles identical to the experiment. Experimental and theoretical yields were normalized to the strongest transition, respectively. Note that the ^{119}Sn$(d,p)^{120}$Sn reaction populates only QPM 1^- states that contain neutron $(3s_{1/2})^{-1}(3p_{1/2})^{+1}$ and $(3s_{1/2})^{-1}(3p_{3/2})^{+1}$ 1p-1h components ([17]).
Bottom: QPM calculations of all $1p-1h$ neutron components related to the PDR in ^{120}Sn

the experimental centroid energy of 6.49 MeV as well as summed (γ,γ') cross-sections for states excited with both probes.

Furthermore, we calculated the branching ratios of the γ-decay from low-energy 1^- states associated with the PDR in ^{120}Sn to the ground- and excited 2^+ states [16]. The obtained results emphasize that the branching ratios serve as a highly sensitive observable for distinguishing between single $p-h$ configurations and multiphonon structures [13, 17].

4 Conclusions

Our nuclear structure approach, which encompasses EDF and three-phonon QPM theory, and more recently, reaction theory, is applied to a wide range of physical systems and processes. The method has proven to be a powerful tool for the systematic investigation of various nuclear excitations at low and higher energies, including pygmy and giant resonances. The predictive power of EDF+QPM theory has been demonstrated in exploratory studies of new nuclear excitations in stable and exotic nuclei, particularly PDR and PQR. The good agreement between the calculated and measured electromagnetic spectral distributions is an indicator of model reliability in the study of nuclear reactions of astrophysical importance. In particular, recent studies of radiation cross sections for neutron and proton capture in N=50 isotons and Pb isotopes provide compelling evidence that the EDF+QPM approach is currently very efficient for such purposes. Furthermore, the EDF+QPM+reaction theory studies of (d,p) and (d,pγ) reactions contribute to the understanding of the microscopic structure of the PDR and its collectivity. This is achieved through unprecedented access to theoretical wave functions that confirm the $1p-1h$ neutron origin of the PDR in these nuclei. Furthermore, knowledge of the microscopic structure of the PDR is shown to be crucial for the precise determination of the (n,γ) reaction rates of key elements of the s- and r-processes of stellar nucleosynthesis.

Acknowledgements

This work is partially supported by the ELI-RO-RDI-2024-AMAP project of the Romanian government.

References

[1] V.G. Soloviev, *Theory of complex nuclei* (Oxford, Pergamon Press, 1976).

[2] V.G. Soloviev, *Theory of atomic nuclei: Quasiparticles and Phonons* (Oxford, Institute of Physics, Bristol, 1992).

[3] M. Grinberg, Ch. Stoyanov, N. Tsoneva, *Physics of Elementary Particles and Atomic Nuclei* **29** (1998) 606-624.

[4] N. Tsoneva, H. Lenske, *Phys. At. Nucl.* **79** (2016) 885-903.

[5] D. Savran, T. Aumann, A. Zilges, *Prog. Part. Nucl. Phys.* **70** (2913) 210-245.

[6] N. Tsoneva, H. Lenske, Ch. Stoyanov, *Phys. Lett. B* **586** (2004) 213-218.

[7] N. Tsoneva, H. Lenske, *Phys. Rev. C* **77** (2008) 024321-024337.

[8] A.P. Tonchev, S.L. Hammond, J.H. Kelley, E. Kwan, H. Lenske, G. Rusev, W. Tornow, N. Tsoneva, *Phys. Rev. Lett.* **104** (2010) 072501-072505.

[9] R. Schwengner, R. Massarczyk, G. Rusev, N. Tsoneva, D. Bemmerer et al., *Phys. Rev. C* **87** (2013) 024306-024318.

[10] A. Bracco, F.C.L. Crespi, E.G. Lanza, *Eur. Phys. J. A* **51** (2015) 99.

[11] A.P. Tonchev, N. Tsoneva, C. Bhatia et al., *Phys. Lett. B* **773** (2017) 20-25.

[12] N. Tsoneva, H. Lenske, *Phys. Lett. B* **695** (2011) 174-180.

[13] N. Tsoneva, M. Spieker, H. Lenske, A. Zilges, *Nucl. Phys. A* **990** (2019) 183-198.

[14] L. Pellegri, A. Bracco, N. Tsoneva et al., *Phys. Rev. C* **92** (2015) 014330-1 - 014330-6.

[15] M. Spieker, N. Tsoneva, V. Derya et al., *Phys. Lett. B* **752** (2016) 102-107.

[16] M. Spieker, A. Heusler, B.A. Brown et al., *Phys. Rev. Lett.* **125** (2020) 102503.

[17] M. Weinert, M. Spieker, G. Potel, N. Tsoneva, M. Müscher, J. Wilhelmy, A. Zilges, *Phys. Rev. Lett.* **127** (2021) 242501.

[18] N. Tsoneva, *Nucl. Phys. A* **1060** (2025) 123114.

[19] P.-A. Söderström, M. Markova, N. Tsoneva et al., *Phys. Rev. C* **112** (2025) 024327.

[20] N. Tsoneva, S. Goriely, H. Lenske, R. Schwengner, *Phys. Rev. C* **91** (2015) 044318-044329.

[21] R. Raut, A.P. Tonchev, G. Rusev et al., *Phys. Rev. Lett.* **111** (2013) 112501-112506.

[22] V.Yu. Ponomarev, Ch. Stoyanov, N. Tsoneva, M. Grinberg, *Nucl. Phys. A* **635** (1998) 470-483.

[23] S. Volz, N. Tsoneva, M. Babilon et al., *Nucl. Phys. A* **779** (2006) 1.

[24] V. Derya, N. Tsoneva, T. Aumann et al., *Phys. Rev. C* **93** (2016) 034311.

[25] J. Isaak, D. Savran, N. Pietralla, N. Tsoneva et al., *Phys. Rev. C* **108** (2023) L051301.

[26] P.-A. Söderström, L. Capponi, E. Açksöz, T. Otsuka, N. Tsoneva, Y. Tsunoda et al., *Nat. Commun.* **11** (2020) 3242.

[27] F. Hofmann, H. Lenske, *Phys. Rev. C* **57** (1998) 2281-2293.

[28] A.I. Vdovin, V.G. Soloviev, *Sov. J. Part. Nucl.* **14** (1983) 237.

[29] M. Grinberg, Ch. Stoyanov, *Nucl. Phys. A* **573** (1994) 231-244.

[30] E.A. McCutchan, A.A. Sonzogni, *Nucl. Data Sheets* **115** (2014) 135-304.

[31] K. Govaert, F. Bauwens, J. Bryssinck et al., *Phys. Rev. C* **57** (1998) 2229.

[32] T. Shizuma, S. Endo, A. Kimura et al., *Phys. Rev. C* **106** (2022) 044326.